Pediatr Radiol (2015) 45:1218–1229
DOI 10.1007/s00247-014-3248-x

PICTORIAL ESSAY

Imaging evaluation of fetal vascular anomalies

Maria A. Calvo-Garcia · Beth M. Kline-Fath · Denise M. Adams · Anita Gupta · Bernadette L. Koch · Foong-Yen Lim · Tal Laor

Received: 4 June 2014 / Revised: 29 September 2014 / Accepted: 17 November 2014 / Published online: 10 December 2014

Abstract Vascular anomalies can be detected in utero and should be considered in the setting of solid, mixed or cystic lesions in the fetus. Evaluation of the gray-scale and color Doppler US and MRI characteristics can guide diagnosis. We present a case-based pictorial essay to illustrate the prenatal imaging characteristics in 11 pregnancies with vascular malformations (5 lymphatic malformations, 2 Klippel-Trenaunay syndrome, 1 venous-lymphatic malformation, 1 Parkes-Weber syndrome) and vascular tumors (1 congenital hemangioma, 1 kaposiform hemangioendothelioma). Concordance between prenatal and postnatal diagnoses is analyzed, with further discussion regarding potential pitfalls in identification.

Keywords Vascular anomalies · Soft-tissue neoplasm · Prenatal diagnosis · Fetal magnetic resonance imaging · Fetal ultrasonography · Children

M. A. Calvo-Garcia (✉) · B. M. Kline-Fath · B. L. Koch · T. Laor
Department of Radiology, MLC 5031
Cincinnati Children's Hospital Medical Center,
3333 Burnet Ave., Cincinnati, OH 45229-3039, USA
e-mail: maria.calvo@cchmc.org

D. M. Adams
Department of Pediatrics and Hemangioma and
Vascular Malformation Center,
Cincinnati Children's Hospital Medical Center,
Cincinnati, OH, USA

A. Gupta
Department of Pathology,
Cincinnati Children's Hospital Medical Center,
Cincinnati, OH, USA

F.-Y. Lim
Pediatric Surgery and Fetal Center of Cincinnati,
Cincinnati Children's Hospital Medical Center,
Cincinnati, OH, USA

Introduction

Vascular anomalies represent the most common cause of pediatric soft-tissue masses [1]. Historically the diagnosis and management of these lesions has been hampered by confusing nomenclature. In 1982, Mulliken and Glowacki [2] devised a simplified classification based on pathology and biological behavior that subsequently was accepted by the International Society for the Study of Vascular Anomalies (ISSVA) in 1996. This vascular anomalies classification scheme clarifies the clinical diagnoses and therapeutic approaches (Fig. 1) [2–4]. Vascular anomalies can be divided into vascular tumors, which are proliferative endothelial lesions with high flow such as hemangiomas, and vascular malformations, which are developmental malformations of hematic or lymphatic vessels.

Vascular malformations are classified as arterial, venous, capillary, lymphatic or mixed (a combination of these) based on their predominant vascular channels. Lesions that have arterial components are termed high-flow malformations whereas anomalies with capillary, lymphatic, or venous components are low-flow malformations [2, 5]. Combined or mixed vascular malformations often are more diffuse than focal abnormalities and can be associated with soft-tissue and skeletal hypertrophy. This group of so-called overgrowth disorders includes lesions composed of high-flow or low-flow components, or a combination of both. Overgrowth can start in utero with low-flow combined lesions such as capillary-lymphatic-venous malformations or with high-flow combined malformations such as capillary-lymphatic-arteriovenous or capillary-venous-arteriovenous malformations [6–8].

Vascular anomalies can compromise vital organs such as the airway or the liver, lead to cardiovascular compromise, or put the fetus at risk for coagulopathies. The possibility of complications from these lesions emphasizes the importance of their detection in utero. In fact, accurate prenatal diagnosis

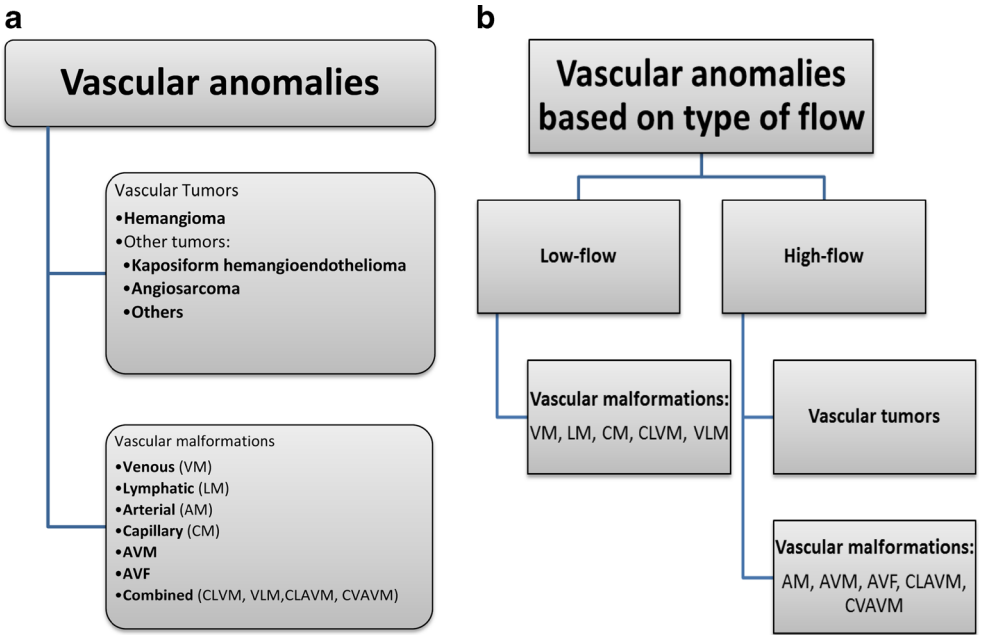

Fig. 1 Clinical and therapeutic approaches to vascular lesions. **a** Classification of vascular anomalies. (Adapted from the International Society for the Study of Vascular Anomalies [4]). **b** Vascular anomalies based on type of flow. *AM* arterial malformation, *AVF* arteriovenous fistula, *AVM* arteriovenous malformation, *CLAVM* capillary-lymphatic-arteriovenous malformation, *CLVM* capillary lymphatic-venous malformation, *CM* capillary malformation, *CVAVM* capillary-venous-arteriovenous malformation, *LM* lymphatic malformation, *VLM* venous-lymphatic malformation, *VM* venous malformation

can improve prenatal care and neonatal outcome [9]. On the other hand, knowledge about these lesions and even their clinical management could be hampered by the persistent use of outdated terminology, which should be abandoned (Table 1) [9, 10].

Materials and methods

This study was approved by the institutional review board, and patient written consent was waived. We performed a retrospective review of 11 children who had a postnatal diagnosis of a vascular anomaly and who had been evaluated prenatally at our institution during a 6-year period. Ten pregnancies were referred for evaluation of masses detected by sonography in the weeks immediately prior to referral. The other pregnancy was referred for additional evaluation based on an initial diagnosis of ventriculomegaly.

Image acquisition

Nineteen level II US and 13 fetal MRI examinations were performed in 11 fetuses at 21 to 35 weeks of gestation (mean 28 weeks). These studies included 11 US and fetal MRI evaluations performed concurrently on the first day of imaging evaluation, and 8 US and 2 MRI examinations performed

Table 1 Clarification of vascular tumor and vascular malformation nomenclature

Old term	Current term (based on lesion composition)
Lymphangioma	Lymphatic malformation
	●Microcystic
Cystic hygroma	●Macrocystic
	●Combined
Cavernous hemangioma (adult liver)	Venous malformation
Vertebral hemangioma (adult spine)	Venous malformation
Orbital cavernous hemangioma (adult orbit)	Venous malformation
	Venous-lymphatic malformation
Central nervous system "cavernoma"	Venous malformation
Cavernous hemangioma, capillary hemangioma, hemangioendothelioma of the liver (infants)	Infantile hemangioma
Klippel-Trenaunay syndrome[a]	Low-flow combined vascular malformation (capillary-lymphatic-venous malformation) with overgrowth
Parkes-Weber syndrome[a]	High-flow combined vascular malformation (capillary-lymphatic-arteriovenous/capillary-venous-arteriovenous malformation) with overgrowth

[a] Note that Klippel-Trenaunay syndrome and Parkes-Weber syndrome are not synonymous, and that Klippel-Trenaunay-Weber syndrome is not an entity [6, 7]

at follow-up evaluation (2–10 weeks from initial imaging). US examinations, which included gray-scale, and color and pulsed Doppler analysis, were performed using an Acuson Sequoia (Siemens Medical Solutions, Malvern, PA) and GE Voluson E8 (GE Medical Systems, Waukesha, WI) equipment. A 2- to 7-MHz multifrequency curvilinear transducer was used (B-mode and color-coded duplex) because the lesions in utero were too deep to allow for evaluation with a higher-frequency linear-array transducer. The Doppler gain was set at 40–50% with low-pulse frequency and a low wall filter, with further adjustments made as needed. Power Doppler technique was used to detect potential vascular areas within the lesion when color Doppler showed no detectable flow.

MRI studies were obtained utilizing a phased-array multichannel body coil in a 1.5-T scanner (Horizon; GE Healthcare, Waukesha, WI). For each fetus, the following sequences were obtained in three orthogonal planes: T2-weighted single-shot fast spin echo (SSFSE), 2-D fast imaging employing steady-state acquisition (FIESTA), and T1-weighted fast spoiled gradient recalled echo (FSPGR). Imaging was obtained using a matrix of 224×192 or 256×256, a field-of-view of 30 cm or less when possible, and 3- to 4-mm-thick contiguous slices (5 mm for FSPGR). No maternal or fetal sedation was utilized. Nine patients had a dedicated fetal echocardiogram as part of their initial evaluation. Three cases had follow-up cardiac exams. We reviewed fetal echocardiogram reports and fetal-maternal and postnatal clinical records.

Image evaluation

All lesions were characterized based on their qualitative color and pulsed Doppler US appearance. A low-flow pattern had no detectable flow, as is expected in a low-flow lesion. A high-flow pattern, as is expected in a high-flow lesion, displayed prominent color flow with arterial waveforms. Doppler US was also used to assess the umbilical cord vessels, the ductus venosus and the middle cerebral artery.

All lesions were also described based on the soft-tissue characteristics on US and fetal MRI as solid, multicystic or mixed. We recorded morphology and extent of each lesion, and effect on adjacent structures, as well as associated findings such as polyhydramnios and hydrops. The heart size was defined by US with the cardiothoracic ratio, measured with the ellipse method at the level of the four chamber-view of the heart during diastole. The cardiothoracic ratio was considered elevated if greater than 0.3 [11]. Fetal cardiac examination included in eight cases the analysis of the combined cardiac output indexed to fetal weight. The combined cardiac output is calculated as (cross-sectional area of aortic valve × velocity time integral of the aortic valve velocity waveform) + (cross-sectional area of pulmonary valve × velocity time integral of the pulmonary valve velocity waveform)] × heart rate [12]. The normal reference range is 425±100 ml/min/kg, with a value of greater than two standard deviations (SD) above the normal combined cardiac output considered elevated (625 ml/min/kg) [13]. Three of the four cases with high-flow pattern had follow-up echocardiograms at our institution to monitor the cardiac function.

Postnatal final diagnoses were assigned after consensus was reached by members of the Hemangioma and Vascular Malformation Center, which includes a dedicated pathologist with expertise in vascular anomalies. Concordance between prenatal and final postnatal diagnoses was determined. These data are summarized in Table 2. We recorded the management of the pregnancy based on the prenatal diagnosis and imaging findings, mode of delivery, as well as neonatal outcome (Table 3).

Results

There was concordance between prenatal and postnatal diagnoses in 8 of 11 cases (73%) whereas three patients (27%) had discordant diagnoses.

Imaging findings in cases with concordant diagnoses

In this category there were six low-flow (cases 1–6) and two high-flow lesions (cases 9 and 11); each followed the expected sonographic flow pattern.

The concordant low-flow lesions included five lymphatic malformations (cases 1–5) and one capillary-lymphatic-venous malformation with overgrowth (also known as Klippel-Trenaunay syndrome) (case 6). These fetuses had normal heart size, normal combined cardiac output and normal Doppler US examination of the umbilical cord vessels, the ductus venosus and the middle cerebral artery.

Four lymphatic malformations (cases 1–4) presented as lateral neck masses with infiltrative trans-spatial margins and a mixed multicystic, avascular appearance (Fig. 2). Two lesions (cases 1 and 2) were very large and were associated with polyhydramnios. The airway was surrounded by or narrowed by the mass in these cases, as seen on fetal MRI. One lymphatic malformation (case 5) presented as a large multicystic avascular mass in the left upper abdomen. On fetal MRI, the mass was intraperitoneal based on its anatomical relationship with adjacent structures, such as the colon. The bowel characteristics and meconium distribution were normal, excluding meconium pseudocyst.

The fetus with the capillary-lymphatic-venous malformation with overgrowth (case 6) presented with diffuse soft-tissue involvement with mixed multicystic and T2-hyperintense lesions in the face, neck, chest wall, superior mediastinum and right axilla along with polyhydramnios.

Table 2 Summary of 11 fetal vascular anomalies. The cases with discordance between prenatal and final postnatal diagnosis are presented in bold

Case #	GA	Prenatal diagnosis	US flow pattern	Lesion tissue characteristics	CTR	CO	Additional fetal MRI findings	Neonatal imaging Prior to treatment/surgery	Pathology analysis	Postnatal diagnosis
1	30	LM	Low-flow	Mixed-multicystic	NL	NL	Compromised airway	No	Yes	LM
2	35	LM	Low-flow	Multicystic	NL	NL	Compromised airway	No	Yes	LM
3	31	LM	Low-flow	Multicystic	NL	NL	Patent airway	Outside CT, same location and multicystic	Yes	LM
4	28	LM	Low-flow	Multicystic	NL	NL	Patent airway	No	Yes	LM
5	31	LM	Low-flow	Multicystic	NL	NC	Normal bowel	US: Low-flow, multicystic	Yes	LM
6	26	KTS	Low-flow	Mixed-multicystic	NL	NC	Compromised airway + Limb hypertrophy	MRI, same distribution, small solid enhancement	Yes	KTS
7	29	Hemimegalencephaly + small **LM**	Low-flow	Solid	NL	NC	Brain findings: consistent with hemimegalencephaly Detection of soft tissue lesion	MRI: Hemimegalencephaly + Chest/abdomen wall low-flow vascular malformation	No, but characteristic skin lesions + hemihypertrophy	**KTS**
8	23	**Cervical teratoma→ Vascular tumor→ Vascular malformation**	**High-flow**	Mixed-solid	↑	↑	Compromised airway	No	Yes (autopsy)	**VLM, mostly venous**
9	25	CH	High-flow	Solid	↑	↑	Normal brain anatomy	No	Yes	CH
10	29	**Sacrococcygeal teratoma**	High-flow	Solid	↑	↑	In retrospect: right buttock (not midline), infiltration of the subcutaneous tissues	No	Yes	**KHE**
11	21	PWS	High-flow	Solid Limb hypertrophy	↑	NL	Patent airway	No	Yes (autopsy)	PWS

CH congenital hemangioma, *CO* combined cardiac output, *CTR* cardiothoracic ratio, ↑ elevated, *GA* gestational age in weeks at workup, *KHE* kaposiform hemangioendothelioma, *KTS* low-flow combined vascular malformation with overgrowth, also known as Klippel-Trenaunay syndrome, *LM* lymphatic malformation, *NC* not calculated, *NL* normal, *VLM* venous-lymphatic malformation, *PWS* high-flow combined vascular malformation with overgrowth, also known as Parkes-Weber syndrome

Table 3 Fetal treatment and outcome of 11 vascular anomalies

Case #	Postnatal diagnosis	Fetal treatment with maternal steroid administration	Type of delivery (gestational age)	Postnatal therapy/outcome
1	LM	No	EXIT to airway (full term)	Surgical resection at 3 days old. Subsequent partial regrowth treated with reoperation and sclerotherapy. Tracheostomy-dependent at present (4 years)
2	LM	No	EXIT to airway (full term)	Surgical resection at 7 days old/partial re-growth with reoperation at 6 months but no airway issues. Subsequently lost to follow-up
3	LM	No	Vaginal (full term)	Sclerotherapy at 7 months and 10 months. No airway issues. Resection at 2 years of age and was doing well 2 months after surgery. Subsequently lost to follow-up
4	LM	No	Cesarean section (placental abruption at 32 weeks)	Sclerotherapy at 1 month followed by 3 rounds of sclerotherapy at 2 years of age and excision 6 months later. No airway issues. After 3 years, lost to follow-up
5	LM	No	Vaginal (35 weeks)	Surgical resection at 1 day old (bilious emesis). Left upper quadrant mesenteric lymphatic malformation found to serve as the lead point for segmental volvulus in proximal jejunum. No complications. Child was 6 years on last unrelated visit to emergency room
6	KTS	No	EXIT to airway (33 weeks)	Debulking of mass around airway at 3 weeks old. Bronchial stent and tracheostomy (still in place at 8 years). Sclerotherapy was followed by surgical excision of axillary component at 3 years old
				Coagulopathy and overgrowth. Under the care of the Hemangioma and Vascular Malformation team
7	KTS	No	Cesarean section (full term with macrocephaly)	Intractable seizures with improvement after functional left hemi-spherotomy at 5 years old.
				Left hemyhypertrophy. Neuromuscular scoliosis status post spinal fusion at 6 years.
				Stable cutaneous lesions
8	VLM, mostly venous	Only for 2 weeks, when a vascular tumor was considered (no response)	EXIT to airway (30 weeks with fetal hydrops)	Disseminated intravascular coagulopathy at birth resulting in death in the first few hours
9	CH	Yes. Tumor decreased in size after 2 weeks, then stable (4 weeks), back to original size at 34 weeks	Cesarean section (36 weeks)	Partially involuting congenital hemangioma, excised at 2 years
10	KHE	No	Cesarean section (35 weeks with cardiac decompensation + maternal mirror syndrome)	Mass resected immediately after birth. No recurrence or residual mass on last visit at 8 months old
11	PWS	No	In utero demise/subsequent induction	Demise

CH congenital hemangioma, *EXIT* ex utero intrapartum treatment, *KHE* kaposiform hemangioendothelioma, *KTS* low-flow combined vascular malformation with overgrowth, also known as Klippel-Trenaunay syndrome, *LM* lymphatic malformation, *PWS* high-flow combined vascular malformation with overgrowth, also known as Parkes-Weber syndrome, *VLM* venous-lymphatic malformation

Right upper limb hypertrophy was depicted well with fetal MRI (Fig. 3).

The two high-flow lesions with concordant postnatal diagnosis included one congenital hemangioma and one capillary-lymphatic-arteriovenous malformation with overgrowth (also known as Parkes-Weber syndrome).

The fetus with a congenital hemangioma (case 9) presented with cardiomegaly, increased combined

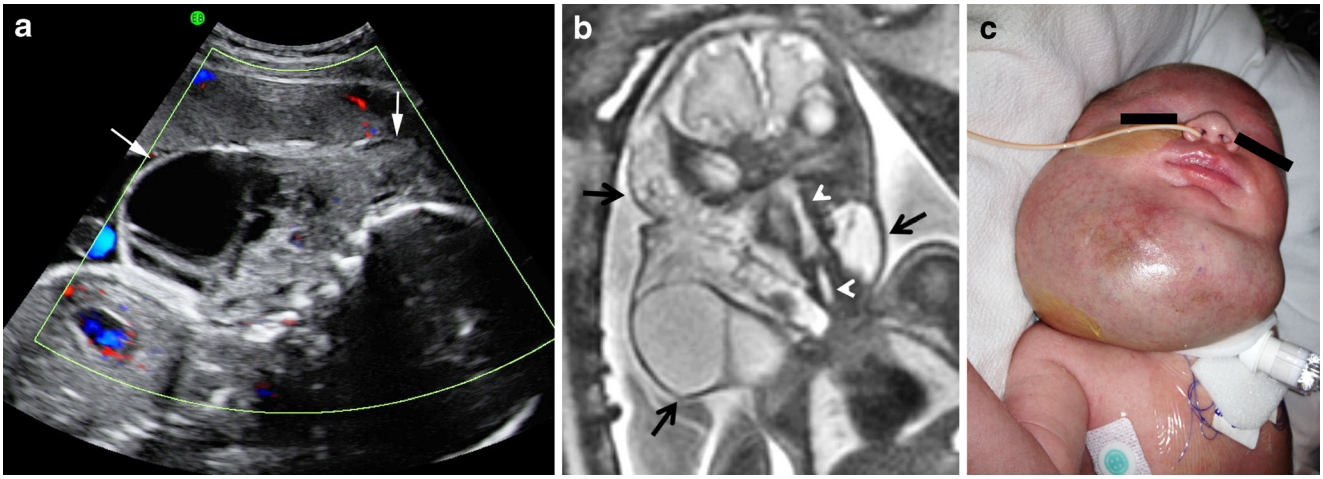

Fig. 2 Case 1. Cervical lymphatic malformation. **a** US with color Doppler and (**b**) fetal MRI coronal SSFSE T2-W image in a 30 weeks' gestational age male fetus. There is a complex, predominantly cystic mass (*arrows*). The airway (*arrowheads*) is well depicted on MRI. **c** Clinical photograph of the mass at 1 day old. *SSFSE* single-shot fast spin echo

cardiac output, normal amniotic fluid volume, and normal Doppler evaluation of the umbilical cord vessels, ductus venosus and middle cerebral artery. The lesion was a well-defined solid posterior neck mass, predominantly echogenic and highly vascular on color Doppler US. Pulsed Doppler US showed low impedance arterial waveforms throughout the mass. On fetal MRI examination, the lesion was intermediate to hyperintense, with numerous flow voids on T2-weighted images, and of intermediate signal intensity on T1-weighted images (Fig. 4). There was no underlying bone remodeling, and MRI evaluation excluded intracranial abnormalities. The mass became more heterogeneous, with scattered non-shadowing echogenic foci, on subsequent sonograms.

The fetus with Parkes-Weber syndrome (case 11) showed right upper extremity enlargement with diffusely heterogeneous solid echogenic soft-tissue thickening and increased vascularity on sonography (Fig. 5). There was involvement of the ipsilateral chest wall and findings included a large right pleural effusion, right lung atelectasis, contralateral mediastinal shift, nuchal and scalp edema, minimal ascites and polyhydramnios. On pulsed Doppler US, low impedance arterial waveforms and pulsatile veins were noted throughout the lesion. There was cardiomegaly, but cardiac output was normal. Fetal Doppler US assessment showed absent end-diastolic flow in the middle cerebral artery and a mildly pulsatile umbilical vein. MRI examination showed diffuse enlargement and soft-tissue thickening of the affected extremity and adjacent chest wall, with hyperintense T2-weighted and hypointense T1-weighted signal, in addition to multiple flow voids. The airway was patent and there was minimal ascites.

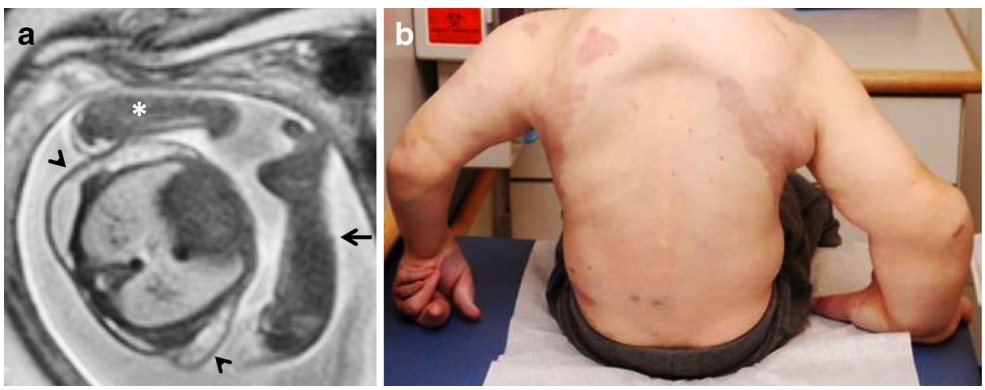

Fig. 3 Case 6. Low-flow capillary-lymphatic-venous malformation with overgrowth (also known as Klippel-Trenaunay syndrome). **a** Fetal MRI axial SSFSE T2-W image in a 26 weeks' gestational age male fetus shows asymmetrical enlargement of the right upper extremity (*arrow*) with increased diameter and muscle bulk. There was extensive infiltration with fluid signal of the soft tissues of the chest wall (*arrowheads*). Normal left forearm (*asterisk*). **b** Clinical photograph of the child at 8 years of age, with corresponding findings. *SSFSE* single-shot fast spin echo

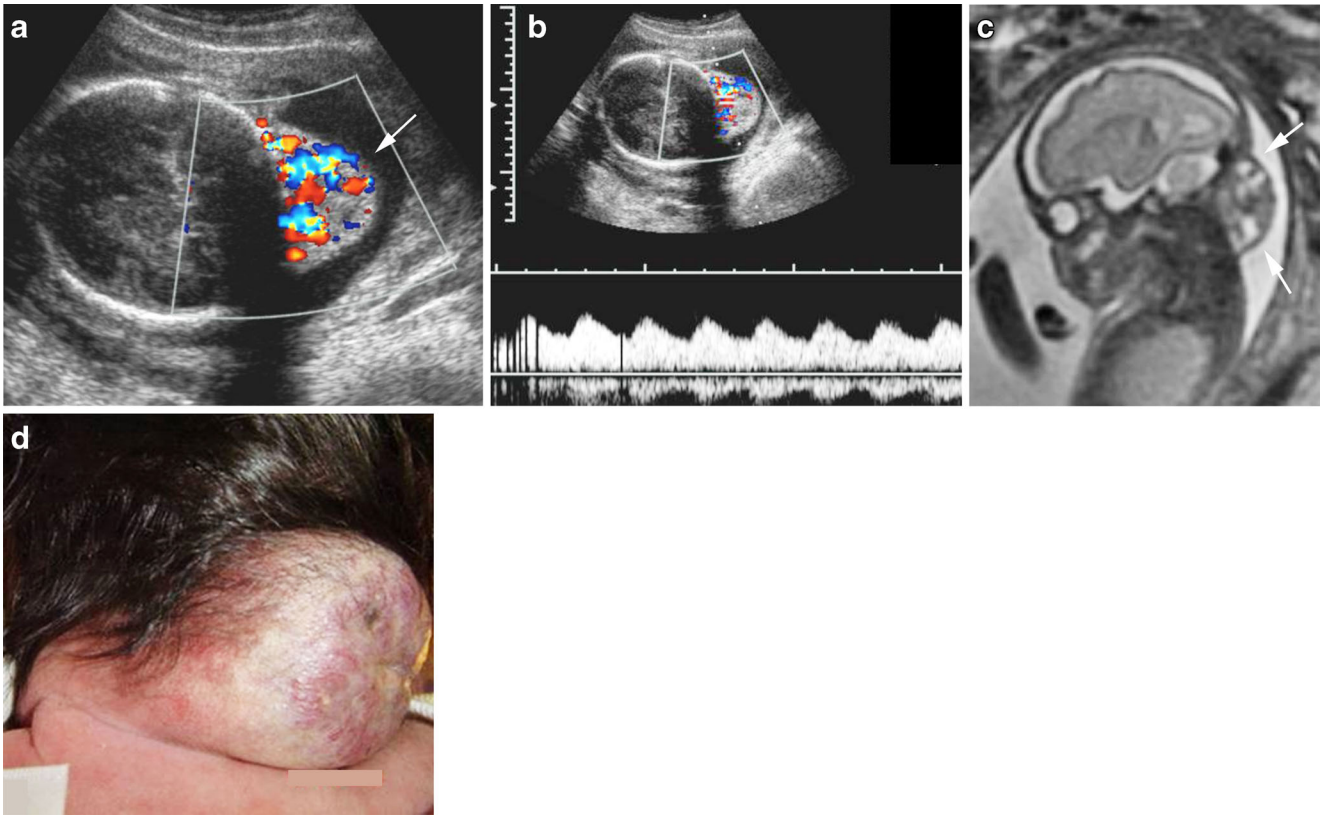

Fig. 4 Case 9. Congenital hemangioma. **a** Axial color Doppler, (**b**) pulsed Doppler US and (**c**) fetal MRI sagittal T2-W images in a 25 weeks' gestational age female fetus. There is a well-defined, solid and hypervascular posterior neck mass (*arrow*) with low-resistance arterial flow. The mass has heterogeneous T2 signal and multiple internal flow voids. **d** Clinical photograph of the mass at birth

Imaging findings in cases with discordant diagnoses

In this category there were two low-flow lesions (cases 7 and 8) and one high-flow lesion (case 10). Cases 7 and 10 followed their expected sonographic flow patterns. However, case 8 presented a high-flow sonographic pattern despite being a low-flow lesion.

The fetus in case 7 was diagnosed with hemimegalencephaly and lymphatic malformation (Fig. 6). The link of these two findings with an overgrowth disorder such as Klippel-

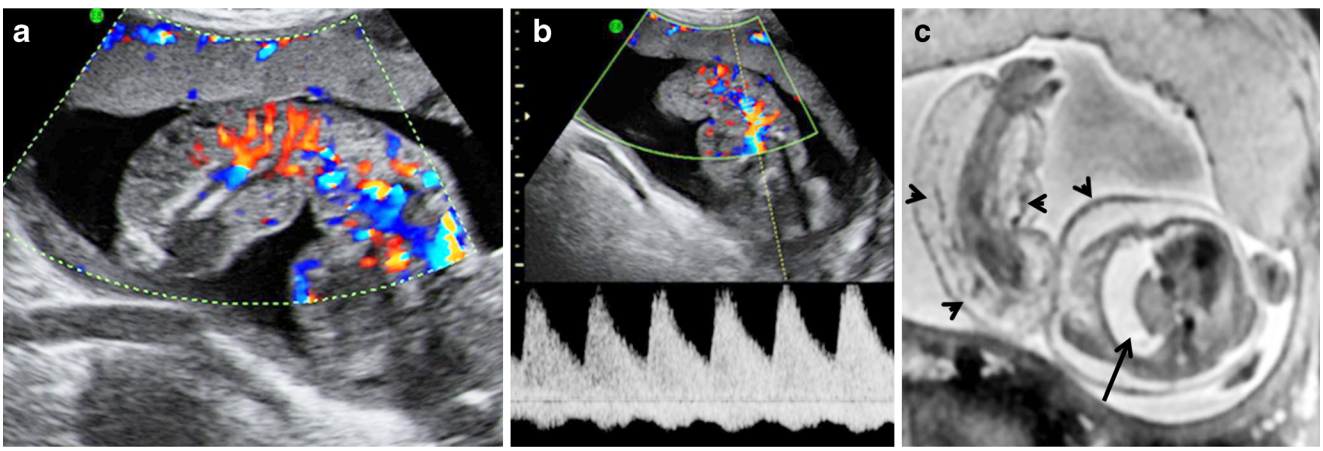

Fig. 5 Case 11. Imaging in a 21-week male fetus with a high-flow combined vascular malformation with overgrowth (also known as Parkes-Weber syndrome). **a** Color Doppler US shows enlargement of the right upper extremity with high-flow pattern. **b** Pulsed Doppler evaluation shows high diastolic arterial flow and pulsatile veins. **c** Axial SSFSE T2-W MR image shows multiple flow voids within the abnormal soft tissues in the right chest wall and upper extremity (*arrowheads*), and moderate to large right pleural effusion (*arrow*). *SSFSE* single-shot fast spin echo

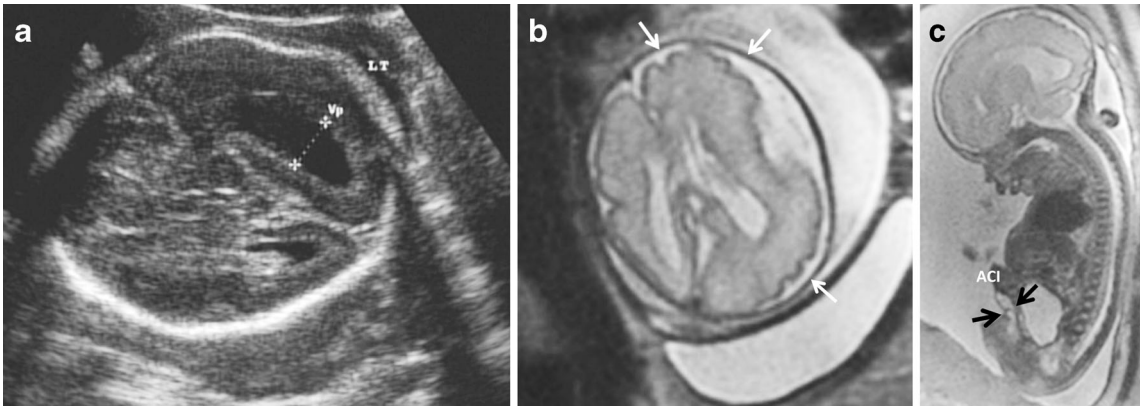

Fig. 6 Case 7. Low-flow combined vascular malformation with hemimegalencephaly in a 29-week male fetus. **a** US gray-scale axial image shows asymmetrical ventriculomegaly (*cursors*). **b** Axial and (**c**) sagittal SSFSE T2-W images show enlargement of the left cerebral hemisphere with abnormal sulcation (*white arrows*) and thickening of the soft tissues (*black arrow*) caudal to the abdominal cord insertion (*ACI*). *SSFSE* single-shot fast spin echo

Trenaunay syndrome was considered only after birth. Fetal MRI characterized the brain findings as hemimegalencephaly and detected focal abdominal wall thickening with hyperintense T2 signal. Subsequent US showed focal abdominal wall solid avascular echogenic thickening. The amniotic fluid volume and Doppler evaluation of the umbilical cord vessels, ductus venosus and middle cerebral artery were normal. The neonate had left-side hemihypertrophy of the face, body and lower extremity, which was not obvious at the time of prenatal imaging evaluation.

In case 10, a kaposiform hemangioendothelioma affected the perineal region of the fetus, with an exophytic appearance that was confused for a solid-type sacrococcygeal teratoma (Fig. 7). The lesion was predominantly echogenic and highly vascular on color Doppler US and showed low impedance arterial waveforms on pulsed Doppler US. On fetal MRI examination, the lesion was intermediate to hyperintense on T2-weighted images and of intermediate signal intensity on T1-weighted images and appeared infiltrative. In addition, unlike a sacrococcygeal teratoma, the lesion was not truly midline. The fetus presented with cardiomegaly and increased combined cardiac output. The amniotic fluid volume and Doppler US examination of the umbilical cord vessels, the ductus venosus and the middle cerebral artery were normal.

Case 8, a venous-lymphatic malformation with a predominant venous component, presented with cardiomegaly in a fetus, increased combined cardiac output and polyhydramnios. The lesion affected the anterior neck and was interpreted initially as a mainly solid-type cervical teratoma. However, upon further review in the days that followed the imaging evaluation, the concern for a vascular tumor such as congenital hemangioma or kaposiform hemangioendothelioma was raised and maternal steroid therapy was started. However, because the lesion almost doubled its volume in 2 weeks a final differential diagnosis of teratoma versus vascular malformation was considered. The lesion was a large, complex, lobulated, predominantly solid and echogenic anterior neck mass (Fig. 8). It had a few scattered cystic foci but no associated calcifications or substantial neck hyperextension. With Doppler US analysis, pulsatile venous and low impedance arterial waveforms were noted in the lesion. The fetal MRI findings correlated with those of the US evaluation. The mass had intermediate T1- and T2-weighted signal intensity with scattered flow voids and areas of hypointense T1 and hyperintense T2 signal. The airway was surrounded by the lesion but not narrowed or displaced.

Discussion

We evaluated a group of fetal vascular anomalies utilizing US and fetal MRI. Gray-scale sonography defined the morphology and consistency of the lesion, while color and spectral Doppler US evaluated the degree of vascularity and determined the type of flow pattern. On sonography we also searched for cardiomegaly and indicators of fetal distress such as polyhydramnios, hydrops and abnormal Doppler of the umbilical cord vessels, ductus venosus and middle cerebral artery. Fetal MRI helped to more precisely define the anatomical location of the mass, to assess integrity of the bowel and to identify potential compromise of vital structures such as the airway.

Following our institutional preference in the setting of a fetal mass or when more than one anomaly is detected, echocardiogram was also done in most of our patients. However, only cases with high-flow lesions would be at risk for high-output congestive heart failure. This complication can be diagnosed in utero by identifying increased blood flow velocities and cardiac output, eventually cardiomegaly, atrioventricular valvular regurgitation and consecutive hydrops [14]. So retrospectively, only patients with high-flow lesions,

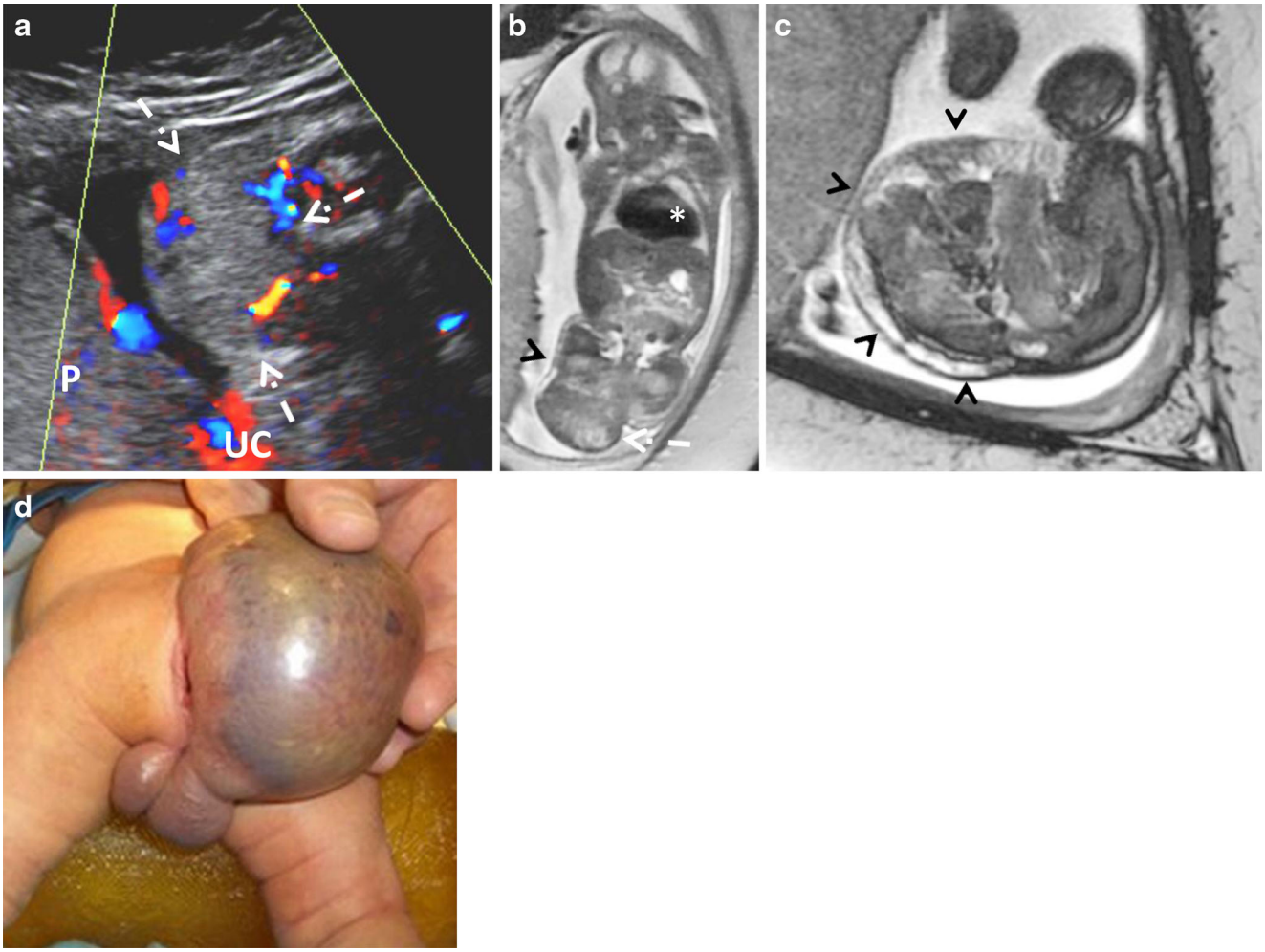

Fig. 7 Case 10. Kaposiform hemangioendothelioma. **a** Coronal color Doppler US image, (**b**) coronal SSFSE T2-W MRI and (**c**) axial 2-D SSFP MR images in a 29 weeks' gestational age female fetus. The buttock mass (*arrows*) is solid and hypervascular on US. MRI shows the eccentric location of the mass and the thickening and infiltration of the subcutaneous fat (*arrowheads*). The heart is enlarged (*asterisk*). Placenta (*P*), and umbilical cord (*UC*) are marked for anatomical reference. **d** Clinical photograph of the mass at birth. *SSFP* steady-state free precession, *SSFSE* single-shot fast spin echo

especially in the presence of cardiomegaly, benefited from this additional exam.

Vascular anomalies can present in multiple locations and can affect not only the soft tissues but also the abdominal and thoracic cavities, as seen in two of our patients. The differential diagnoses in the presence of a fetal soft-tissue mass are guided by the sonographic flow pattern (Fig. 1) and are presented in Table 4.

A low-flow vascular pattern is expected in venous, capillary and lymphatic malformations, as well as in their combined forms (Fig. 1) [15]. All our cases of capillary-lymphatic-venous malformation with overgrowth (also known as Klippel-Trenaunay syndrome) and lymphatic malformations presented this vascular pattern in utero, in concordance with prior reports [16–18]. In addition, the heart size and combined cardiac output were normal. Lymphatic malformations are more frequently found in the neck and axillary regions and represent the most commonly diagnosed fetal vascular malformation [9, 19]. They can have a multicystic, mixed or solid appearance with infiltrative margins, and are characterized by trans-spatial involvement when they occur in the head and neck, as in our series [7]. The main differential diagnosis, especially when the lesion involves the neck or perineum, is a cystic teratoma [9]. However teratomas typically have relatively well-defined margins, can contain calcifications, have vascularity that can be readily identified in their solid portions, and are typically centered along the midline such as the anterior neck or coccyx. Both lymphatic malformations and cervical teratomas can compromise the airway, have a potential risk for bleeding, and might require the same clinical approach at the time of the delivery through an ex utero intrapartum treatment (EXIT) to airway procedure [20]. In the abdomen, the mesentery of the small bowel is also a frequent location for lymphatic malformation. A previous case with this diagnosis was misinterpreted as bowel perforation prenatally [9]. Fetal MRI in one of our patients allowed for

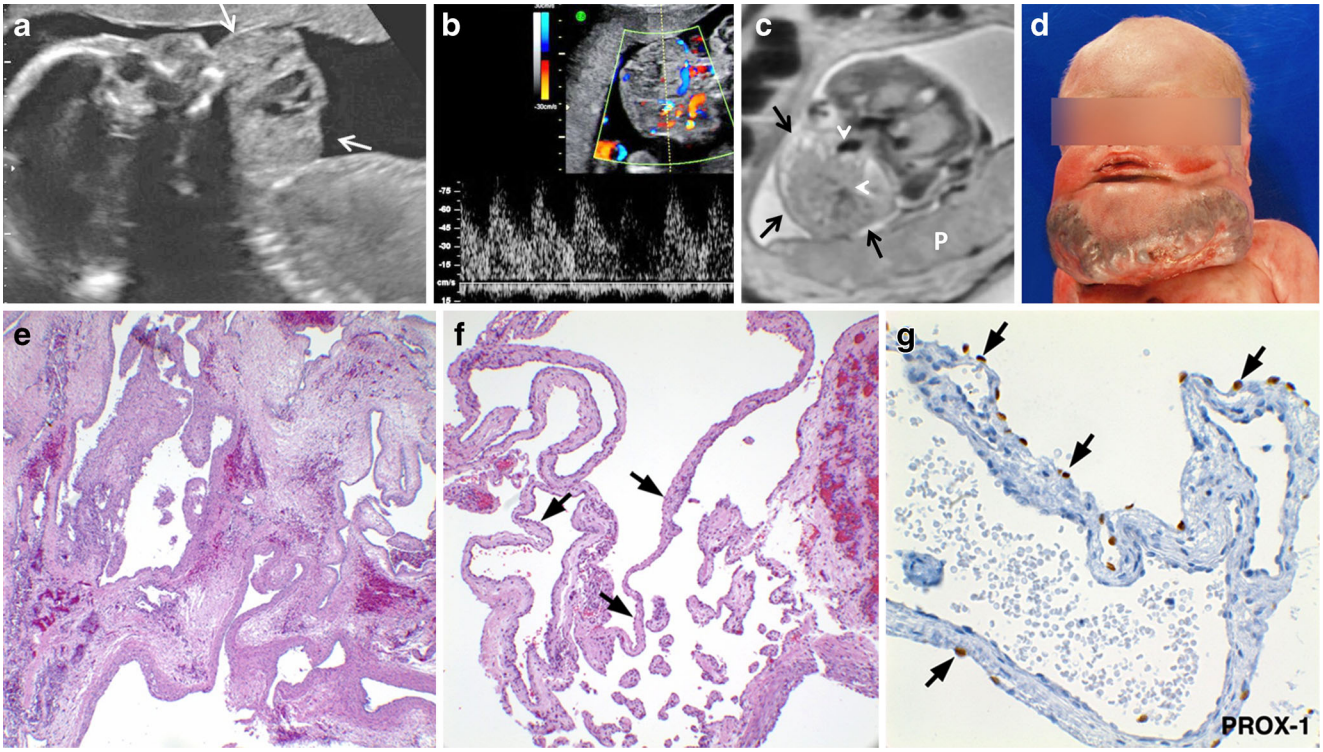

Fig. 8 Case 8. Cervical venous-lymphatic malformation in a 23-week male fetus. **a** Sagittal gray-scale US image and (**b**) axial pulsed Doppler image show a predominantly solid mass (*arrows*) with high-flow pattern. **c** Fetal MRI axial SSFSE T2-W image. At the base of the mass (*arrows*), flow voids (*arrowheads*) are noted. Placenta (P). **d** Clinical photograph of the lesion at birth. **e** Histology demonstrates a soft-tissue and muscular vascular lesion composed primarily of an excessive number of medium-size malformed veins with concentric smooth muscle within the wall. The endothelial cells are flattened (hematoxylin and eosin stain x100). **f** There are occasional small- to medium-size malformed vascular channels lined by single layer of round endothelial cells (*arrows*) with partial to no smooth muscle within the walls (hematoxylin and eosin stain x100). **g** Immunostain for PROX-1, a lymphatic endothelial marker, is immunoreactive in the endothelial cells (*arrows*) of the lymphatic channels. PRO-1 immunostain x200 (*brown*). *SSFSE* single-shot fast spin echo

determination of the lesion's anatomical location and for confirmation of the normal appearance of adjacent structures, which included the bowel.

The imaging characteristics of the lesions in the cases of Klippel-Trenaunay syndrome resembled those of the lymphatic malformations. The clue to the correct diagnosis in one of

Table 4 Differential diagnosis guide for a fetal soft-tissue lesion

Differential diagnosis	Pulsed Doppler US findings
Low-flow sonographic pattern	No detectable flow
a) Low-flow vascular malformations	
1. Classic pattern for LM, VLM, VM and CM	
2. Combined low-flow vascular malformation with limb hypertrophy or hemimegalencephaly	
b) Other lesions, e.g., cystic teratoma, dermoid cyst	
High-flow sonographic pattern	
a) Vascular tumors: congenital hemangioma, kaposiform hemangioendothelioma	Low impedance arterial flow
b) Tumors with vascular appearance: teratoma, congenital-infantile fibrosarcoma, infantile myofibromatosis	Low impedance arterial flow
c) High-flow vascular malformations	Low impedance arterial flow and pulsatile veins
1. AVF, AVM (no mass associated)	
2. Combined high-flow vascular malformation with limb hypertrophy	
d) Low-flow vascular malformation simulating a high-flow lesion (such as VLM in our series)	Low impedance arterial flow

AVF ateriovenous fistula, *AVM* arteriovenous malformation, *CM* capillary malformation, *LM* lymphatic malformation, *VLM* venous-lymphatic malformation, *VM* venous malformation

the two cases was the extensive involvement of the soft tissue in multiple areas in association with limb hypertrophy. In the second case, there was no detectable overgrowth in utero and the soft-tissue lesion was small. However the fetal MRI characterized the brain findings as hemimegalencephaly, a rare disorder that has been described in isolation or in association with these vascular malformations [21, 22]. The reported findings include macrocephaly, asymmetrical enlargement of one cerebral hemisphere, ipsilateral ventriculomegaly and gyral disorganization [23].

A particularly challenging case in our series was a very large venous-lymphatic malformation with a predominantly venous component (case 8) that presented with a high-flow vascular pattern, increased combined cardiac output and cardiomegaly. It involved the anterior neck and was initially thought to represent a cervical teratoma, although the lack of significant mass effect and neck hyperextension was evidence against that diagnosis. Subsequently the diagnosis of a vascular anomaly was considered. The coagulopathy present at birth and the physical examination were characteristic of a large venous malformation [24]. However no arterial components or arteriovenous connections were found on pathological analysis to explain the high-flow vascular appearance on imaging. Venous-lymphatic and venous malformations are low-flow lesions that contain anomalous venous lakes and channels. The expected internal sluggish flow usually translates to no detectable flow with color or pulsed Doppler US [7]. A prenatal report of venous-lymphatic malformation showed this low-flow pattern without detectable vascularity using color Doppler US [25]. We are not aware of previous reports on prenatal pure venous malformations with which to compare the characteristics of our case. In fact, we can only partially explain our discrepant high-flow pattern based on anatomical features. Potential explanations include that a very large venous malformation could demand substantial blood supply, or that the arteriolar flow that feeds the malformation might be detected within the septa or at the periphery of the lesion, although the flow seemed out of proportion to this explanation in our patient [7]. In addition, these malformations can communicate directly with the venous system, which explains why we also noted dilatation of the jugular vein and venous flow with spectral characteristics similar to the pulsatile jugular vein waveforms [15]. We suspect that in addition to the large size of this mass, the coagulopathy present with this malformation and the hormonal in utero environment could have altered the fetal hemodynamics.

The remaining cases with a high-flow vascular pattern and cardiomegaly correlated with high-flow lesions (Fig. 1). Vascular tumors in our series included congenital hemangioma and kaposiform hemangioendothelioma, both of which were solid soft-tissue masses with prominent color flow and dominant low-resistance arterial waveforms. Congenital hemangioma was the more vascular of the two considerations based on color Doppler US characteristics and was correctly diagnosed in utero. Imaging features in our patient were concordant with prior prenatal reports [26, 27]. On the other hand, the diagnosis of kaposiform hemangioendothelioma was not suspected prospectively. Instead, the lesion was thought to represent a solid sacrococcygeal teratoma, because this is a more frequent fetal mass with a similar hypervascular appearance and anatomical location. On retrospective review, the MRI examination of our patient showed an eccentric perineal lesion, which extended from the right buttock area instead of from the midline as would be expected for a teratoma. This is an important clue, because the proximal portion of the limbs and the trunk are the areas most frequently involved by this vascular tumor [24]. We also noted thickening and infiltration of the subcutaneous fat in the proximal portion of the lesion. This has been described as a highly characteristic feature of kaposiform hemangioendothelioma on postnatal MRI and might also have guided our diagnosis [6, 28].

Other soft-tissue tumors that present in the fetal-neonatal period with a hypervascular appearance include infantile myofibromatosis and congenital infantile fibrosarcoma [29, 30]. However these tumors have not been described in association with cardiomegaly or congestive heart failure. Vascular tumors can be differentiated from high-flow vascular malformations. An arteriovenous fistula or arteriovenous malformation shows high-flow vessels on color Doppler US and pulsatile veins and high diastolic arterial waveforms on pulsed Doppler US and usually lacks an associated soft-tissue mass. This imaging pattern did not fit with any of the vascular tumors in our cohort and thus these high-flow vascular malformations were not considered in the differential diagnosis [6]. In case 11, the capillary-lymphatic-arteriovenous malformation with overgrowth (also known as Parkes-Weber syndrome), the diagnosis was supported by the presence of hypervascularity of the involved tissues, signs of arteriovenous connections throughout the lesion on pulsed Doppler US and associated limb hypertrophy [31]. In this setting, the soft tissues are abnormal, unlike in an arteriovenous fistula or arteriovenous malformation.

The limitations of our analysis include the retrospective nature and small number of cases. However, we believe that the observations we provide may be helpful to other physicians who evaluate fetal masses and might improve the accuracy of diagnosis, the counseling and the management of future pregnancies. Awareness of the prenatal imaging appearance of vascular anomalies and careful evaluation of these lesions could serve to avoid confusion with other lesions, such as teratomas. Overall the in utero US flow pattern guides the

diagnostic approach and is complemented by MRI, as well as fetal echocardiography in cases of high-flow lesions. We expect that future experience will provide further insight to these lesions.

Conflicts of interest None

References

1. Navarro OM, Laffan EE, Ngan BY (2009) Pediatric soft-tissue tumors and pseudo-tumors: MR imaging features with pathologic correlation: part 1. Imaging approach, pseudotumors, vascular lesions, and adipocytic tumors. Radiographics 29:887–906
2. Mulliken JB, Glowacki J (1982) Hemangiomas and vascular malformations in infants and children: a classification based on endothelial characteristics. Plast Reconstr Surg 69:412–422
3. Kollipara R, Dinneen L, Rentas KE et al (2013) Current classification and terminology of pediatric vascular anomalies. AJR Am J Roentgenol 201:1124–1135
4. International Society for the Study of Vascular Anomalies (2014) ISSVA classification updates. http://www.issva.org/content.aspx?page_id=22&club_id=298433&module_id=152904
5. Fishman SJ, Mulliken JB (1993) Hemangiomas and vascular malformations of infancy and childhood. Pediatr Clin N Am 40: 1177–1200
6. Behr GG, Johnson C (2013) Vascular anomalies: hemangiomas and beyond — part 1, fast-flow lesions. AJR Am J Roentgenol 200:414–422
7. Behr GG, Johnson CM (2013) Vascular anomalies: hemangiomas and beyond — part 2, slow-flow lesions. AJR Am J Roentgenol 200: 423–436
8. Biesecker LG, Happle R, Mulliken JB et al (1999) Proteus syndrome: diagnostic criteria, differential diagnosis, and patient evaluation. Am J Med Genet 84:389–395
9. Marler JJ, Fishman SJ, Upton J et al (2002) Prenatal diagnosis of vascular anomalies. J Pediatr Surg 37:318–326
10. Hassanein AH, Mulliken JB, Fishman SJ et al (2011) Evaluation of terminology for vascular anomalies in current literature. Plast Reconstr Surg 127:347–351
11. Awadh AM, Prefumo F, Bland JM et al (2006) Assessment of the intraobserver variability in the measurement of fetal cardiothoracic ratio using ellipse and diameter methods. Ultrasound Obstet Gynecol 28:53–56
12. Kenny JF, Plappert T, Doubilet P et al (1986) Changes in intracardiac blood flow velocities and right and left ventricular stroke volumes with gestational age in the normal human fetus: a prospective Doppler echocardiographic study. Circulation 74: 1208–1216
13. Mielke G, Benda N (2001) Cardiac output and central distribution of blood flow in the human fetus. Circulation 103:1662–1668
14. Mejides AA, Adra AM, O'Sullivan MJ et al (1995) Prenatal diagnosis and therapy for a fetal hepatic vascular malformation. Obstet Gynecol 85:850–853
15. Eivazi B, Fasunla AJ, Hundt W et al (2011) Low flow vascular malformations of the head and neck: a study on brightness mode, color coded duplex and spectral Doppler sonography. Eur Arch Otorhinolaryngol 268:1505–1511
16. Goncalves LF, Rojas MV, Vitorello D et al (2000) Klippel-Trenaunay-Weber syndrome presenting as massive lymphangiohemangioma of the thigh: prenatal diagnosis. Ultrasound Obstet Gynecol 15:537–541
17. Rasidaki M, Sifakis S, Vardaki E et al (2005) Prenatal diagnosis of a fetal chest wall cystic lymphangioma using ultrasonography and MRI: a case report with literature review. Fetal Diagn Ther 20:504–507
18. Moukaddam H, Pollak J, Haims AH (2009) MRI characteristics and classification of peripheral vascular malformations and tumors. Skelet Radiol 38:535–547
19. Robson CD, Barnewolt CE (2004) MR imaging of fetal head and neck anomalies. Neuroimaging Clin N Am 14:273–291
20. Kathary N, Bulas DI, Newman KD et al (2001) MRI imaging of fetal neck masses with airway compromise: utility in delivery planning. Pediatr Radiol 31:727–731
21. Papetti L, Tarani L, Nicita F et al (2012) Macrocephaly-capillary malformation syndrome: description of a case and review of clinical diagnostic criteria. Brain Dev 34:143–147
22. Vurucu S, Battal B, Kocaoglu M et al (2009) Klippel-Trenaunay syndrome with hemimegalencephaly, retroperitoneal lymphangioma and double inferior vena cava. Br J Radiol 82:e102–e104
23. Alvarez RM, Garcia-Diaz L, Marquez J et al (2011) Hemimegalencephaly: prenatal diagnosis and outcome. Fetal Diagn Ther 30:234–238
24. Marler JJ, Mulliken JB (2005) Current management of hemangiomas and vascular malformations. Clin Plast Surg 32:99–116
25. Sherer DM, Perenyi AR, Glick SA et al (2006) Prenatal sonographic findings of extensive low-flow mixed lymphatic and venous malformations. J Ultrasound Med 25:1469–1473
26. Elia D, Garel C, Enjolras O et al (2008) Prenatal imaging findings in rapidly involuting congenital hemangioma of the skull. Ultrasound Obstet Gynecol 31:572–575
27. Kaplan MC, Coleman BG, Shaylor SD et al (2013) Sonographic features of rare posterior fetal neck masses of vascular origin. J Ultrasound Med 32:873–880
28. Croteau SE, Liang MG, Kozakewich HP et al (2013) Kaposiform hemangioendothelioma: atypical features and risks of Kasabach-Merritt phenomenon in 107 referrals. J Pediatr 162:142–147
29. Boon LM, Fishman SJ, Lund DP et al (1995) Congenital fibrosarcoma masquerading as congenital hemangioma: report of two cases. J Pediatr Surg 30:1378–1381
30. Kubota A, Imano M, Yonekura T et al (1999) Infantile myofibromatosis of the triceps detected by prenatal sonography. J Clin Ultrasound 27:147–150
31. Ziyeh S, Spreer J, Rossler J et al (2004) Parkes Weber or Klippel-Trenaunay syndrome? Non-invasive diagnosis with MR projection angiography. Eur Radiol 14:2025–2029